Int J Earth Sciences (Geol Rundsch) (2001) 90:136–148
DOI 10.1007/s005310000148

ORIGINAL PAPER

Holger Stünitz · Jan Tullis

Weakening and strain localization produced by syn-deformational reaction of plagioclase

Received: 9 November 1999 / Accepted: 9 October 2000 / Published online: 8 December 2000

Abstract There are many observations in naturally deformed rocks on the effects of mineral reactions on deformation, but few experimental data. In order to study the effects of chemical disequilibrium on deformation we have investigated the hydration reaction plagioclase + H_2O → more albitic plagioclase + zoisite + kyanite + quartz. We utilized fine-grained (2–6 μm) plagioclase aggregates of two compositions (An54 and An60), both dried and with 0.1–0.4 wt% H_2O present, in shear deformation experiments at two sets of conditions: 900 °C, 1.0 GPa (in the plagioclase stability field) and 750 °C, 1.5 GPa (in the zoisite stability field). Dry samples and those deformed in the plagioclase stability field underwent homogeneous shearing by dislocation creep, but samples with 0.1 to 0.4 wt% water deformed in the zoisite stability field showed extreme strain localization into very narrow (~1–3 μm) shear bands after low shear strain. In these samples the microstructures of reaction products in the matrix differ from those in the shear bands. In the matrix, large (up to 400 μm) zoisite crystals grew in the direction of finite extension, and relict plagioclase grains are surrounded by rims of recrystallized grains that are more albitic. In the shear bands, the reaction products albitic plagioclase, zoisite, white mica, and traces of kyanite form polyphase aggregates of very fine-grained (<0.1 μm) dislocation-free grains. Most of the sample strain after γ ~2 has occurred within the shear bands, within which the dominant deformation mechanism is inferred to be diffusion-accommodated grain boundary sliding (DAGBS). The switch from dislocation creep in dry samples deformed without reaction to DAGBS in reacted samples is associated with a decrease in flow stress from ~800 to <200 MPa. These experiments demonstrate that heterogeneous nucleation driven in part by chemical disequilibrium can produce an extremely fine-grained polyphase assemblage, leading to a switch in deformation mechanism and significant weakening. Thus, localization of deformation in polyphase rocks may occur on any pressure (P),temperature (T)-path where the equilibrium composition of the constituent minerals changes.

H. Stünitz (✉)
Department of Earth Sciences, Basel University,
Bernoullistr. 32, 4056 Basel, Switzerland
Phone: +41-61-2673596
Fax: +41-61-2673613

J. Tullis
Department of Geological Sciences, Brown University,
Providence, RI 02912, USA

Introduction

Polyphase rocks make up most of the lithosphere, but their deformation behavior is poorly understood. Most theoretical models of the rheology of polyphase rocks assume that all constituent phases deform by the same dominant deformation mechanism and that the mechanism does not change during the deformation history (e.g., Handy 1990; Tullis et al. 1991). Experimental investigations and modeling of such systems indicate that for dislocation creep, the strength of a two-phase rock is always between the upper and lower bounds of the constituent phases. The strength of such an aggregate varies in a non-linear way with composition, and usually is close to that of the weaker phase if more than ~20% of this phase is present (e.g., Jordan 1987; Handy 1990; Tullis and Wenk 1994). Only for diffusion creep deformation do models predict that the strength of a two phase aggregate can be lower than that of both end members (Wheeler 1992; Fueten and Robin 1992).

In most experimental deformation studies to date on polyphase aggregates the phases were in chemical equilibrium. However, during the deformation history in most tectonic settings (crustal thinning, subduction, obduction and erosion), the deforming rock masses

move along pressure (P),temperature (T) paths. Most rock-forming minerals are solid solutions, and their equilibrium composition in a given assemblage changes as the P,T conditions change. Thus, the free energy of the deforming minerals changes not only because of the deformation itself (stored strain energy in the form of dislocations), but also because of chemical disequilibrium (e.g., Evans et al. 1986; Hay and Evans 1987a,1987b; Cumbest et al. 1989; Stünitz 1998; Newman et al. 1999). The recrystallization and/or neocrystallization of these minerals during deformation commonly produces new phases; new phases may be heterogeneously nucleated or existing phases may change their composition. If new phases nucleate during deformation, weakening may occur by four possible mechanisms:

1. The new phases may be mechanically weak (e.g., Mitra 1978; White and Knipe 1978; Rubie 1990a).
2. The fine grain size of the new phases may allow the deformation mechanism to change to diffusion-accommodated grain boundary sliding (e.g., Boullier and Gueguen 1975; Kerrich et al. 1980; Rubie 1983, 1990a; Rutter and Brodie 1988a,1988b; Fitz Gerald and Stünitz 1993; Stünitz and Fitz Gerald 1993; Newman et al. 1999).
3. During dehydration reactions, the pore pressure may increase and lead to brittle failure. The effects of dehydration reactions have been investigated experimentally (Raleigh and Paterson 1965; Murrell and Ismael 1976; Olgaard et al. 1995). In experiments under drained conditions, the weakening effect is not pronounced or only transient.
4. Transformation plasticity may occur during the reaction process (Poirier 1982; Meike 1993).

Pore pressure effects and transformation plasticity are likely to produce only transient weakening. New phases that are weak and grain size reduction are probably geologically more important; examples of such effects are summarized by Handy (1989) and Rubie (1990a).

We undertook an experimental study of the possible weakening effects of a hydration reaction that occurs during viscous deformation. Studying a hydration reaction allowed us to avoid weakening caused by embrittlement resulting from pore fluid pressure, because the pore pressure decreases during the experiment. Deformation experiments were carried out on intermediate plagioclase both at equilibrium conditions (900 °C, 1 GPa) and at disequilibrium conditions (750 °C, 1.5 GPa), where intermediate plagioclase reacts with H_2O to produce zoisite and more albitic plagioclase and other phases (Fig. 1a). We avoided P,T conditions where incongruent melting of plagioclase occurs. Previous deformation experiments on albite indicate that plagioclase, if chemically stable, should be very strong at 750 °C, 1.5 GPa because of limited crystal plasticity (Tullis and Yund 1992). However, at 900 °C, 1.0 GPa, the dominant deformation mechanism in albite and intermediate plagioclase is

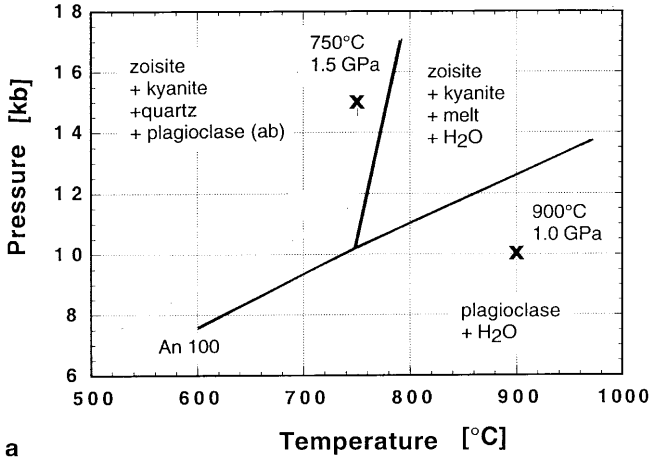

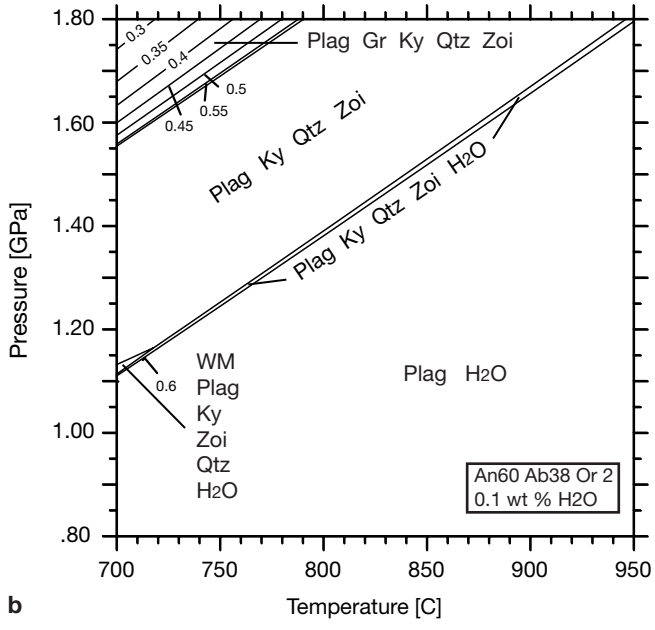

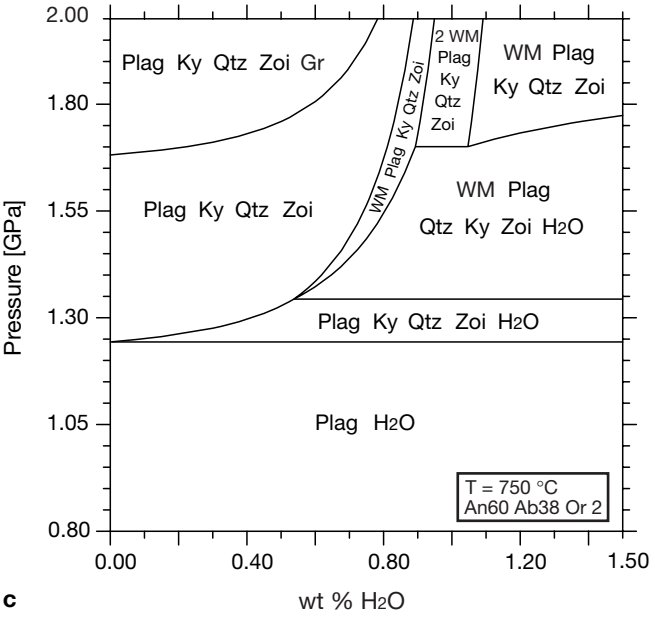

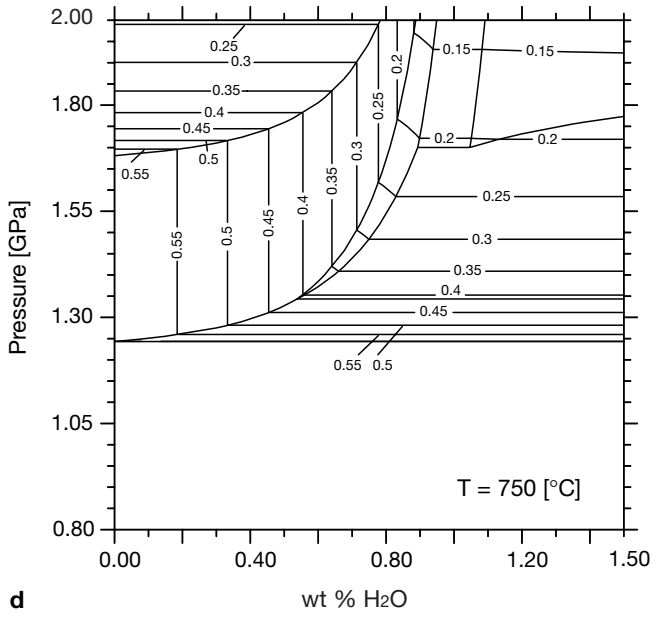

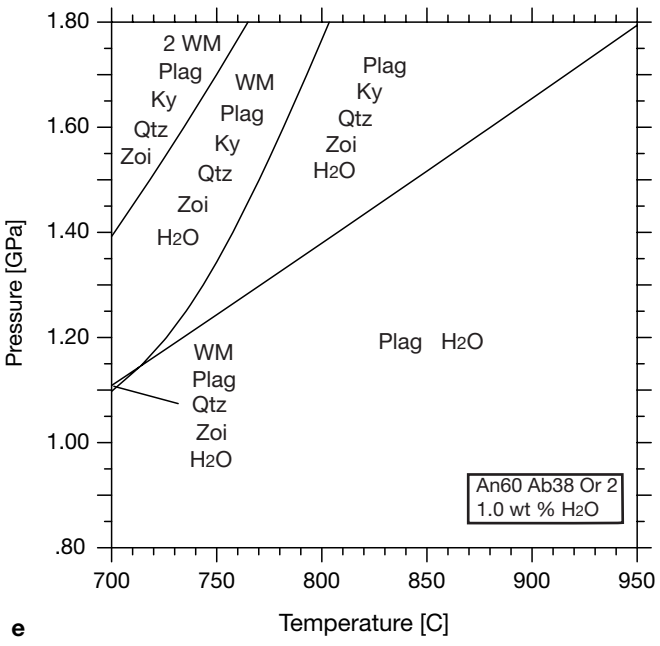

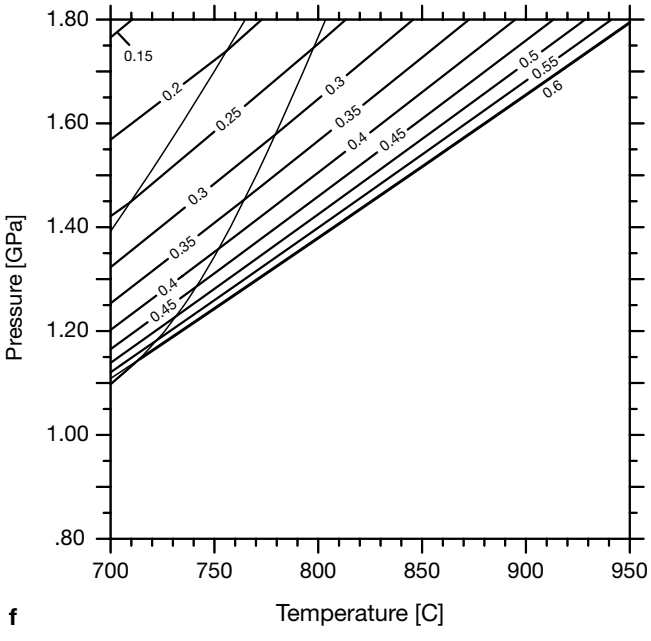

Fig. 1 Phase and pseudobinary diagrams of the system: plagioclase $+H_2O$. **a** Experimentally determined plagioclase phase diagram after Goldsmith (1982). *Solid lines* are extrapolated stabilities for anorthite + H_2O → zoisite + kyanite + quartz. The *crosses* mark the two sets of conditions under which our experiments have been carried out: 750 °C, 1.5 GPa (zoisite stability field) and 900 °C, 1.0 GPa (intermediate plagioclase stability field). P, T conditions where plagioclase undergoes incongruent melting of the anorthite component had to be avoided in our experiments. **b** P,T diagram calculated for a plagioclase composition An60–Ab38–Or2, (corresponding to the Sonoran (An60) starting material, see analysis in Table 1) at 0.1 wt% H_2O (approximately the amount of H_2O present in the "as-is" sample of An60). Isopleths are contoured for An-content of the equilibrium plagioclase. The equilibrium plagioclase composition at 750 °C, 1.5 GPa is An57. **c** Pseudobinary diagram calculated for a plagioclase composition An60–Ab38–Or2 at 750 °C for different pressures and H_2O contents. The fields with H_2O as a stable phase indicate H_2O-saturated conditions, where not all H_2O is used up in the reaction. *WM* K-mica; *2 WM* K-mica and a Na-mica. **d** Isopleths for **c**, showing the anorthite content of the equilibrium plagioclase phase. **e** P,T diagram calculated for a plagioclase composition An60–Ab38–Or2, at 1.0 wt% H_2O, which is approximately the H_2O content that is required to react the whole sample starting material (corresponding to H_2O-saturated conditions). *WM* K-mica; *2 WM* K-mica and Na-mica. **f** Isopleths for **e**, showing the anorthite content of the equilibrium plagioclase phase. At 750 °C, 1.5 GPa, the anorthite content of the stable plagioclase is An29

recrystallization-accommodated dislocation creep (regime 1 of Hirth and Tullis 1992), and strengths are significantly lower than at 750 °C for strain rates of 10^{-5} to 10^{-6} s^{-1} (Tullis and Yund 1985; Tullis et al. 1990). Zoisite (or epidote, clinozoisite) appears to be stronger than plagioclase over a wide range of conditions. Epidote group minerals usually form undeformed porphyroclasts and dislocation-free grains in rocks naturally deformed at greenschist facies conditions (Stünitz 1993; Stünitz and Fitz Gerald 1993), and to our knowledge no examples of plastic deformation of these minerals, even at high temperatures, have been described in the literature. Therefore, if there is no switch in deformation mechanism, the formation of zoisite should result in a flow stress for the two phase plagioclase–zoisite aggregate that is higher than that of the plagioclase end-member (although for very small amounts of zoisite, the effect could be negligible). However, if the reaction results in a flow stress significantly lower than that of plagioclase, it is most likely that the dominant deformation mechanism changed.

Table 1 Composition of plagioclase starting materials

	Sonoran disordered Labradorite		Schiller ordered Labradorite	
	(wt%)	Atoms per 8 oxygens	(wt%)	Atoms per 8 oxygens
SiO_2	53.01	2.398	54.92	2.458
Al_2O_3	29.83	1.590	29.84	1.566
FeO	0.36	0.013	0.08	0.003
CaO	12.49	0.605	10.94	0.522
Na_2O	4.30	0.378	5.00	0.432
K_2O	0.30	0.017	0.50	0.028
Total	100.29	5.001	101.26	5.009
		An60 Ab38 Or2		An54 Ab44 Or2

The phase diagram for the system plagioclase + H_2O was calculated using the program DOMINO, created by de Capitani and Brown (1987) and de Capitani (1994), using the Berman (1988) database, the plagioclase solution model of Fuhrman and Lindsley (1988), and the mica solution model of Chatterjee and Froese (1975). This program uses a bulk chemical composition as input. A phase diagram (Fig. 1b) was first calculated for one of the starting materials (gem-quality plagioclase An60, Table 1) and the actual H_2O content of the experiments (0.1 wt% H_2O; (Fig. 1b). In Fig. 1b, the isopleths (An content of plagioclase) for the bulk composition of the plagioclase sample (An60) indicate that there is only a minor change in the equilibrium anorthite content at 0.1 wt% H_2O because of the small amount (~3 mol%) of zoisite formed by the reaction (Goldsmith 1982):

4 anorthite + 1 H_2O → 2 zoisite + 1 kyanite + 1 quartz

However, for higher H_2O contents, there is a change not only in the modal amount of the reaction products and their composition but also in the phase assemblage, as shown by the calculated pseudo-binary pressure-H_2O-diagram (Fig. 1c). For H_2O contents >0.8 wt% in the system plagioclase (An60)+H_2O, white mica becomes a stable phase (largely K-mica because of the orthoclase component of the plagioclase, Table 1) and the equilibrium bulk anorthite component of the plagioclase changes considerably because of the greater amount (~21 mol%) of zoisite formed (Fig. 1c,d). Thus, the H_2O content of the system controls the phase assemblage, as well as the modal amount and composition of product phases. We found this factor to be important in our experiments because locally there were higher H_2O contents.

Experimental and analytical procedures

Simple shear deformation experiments were carried out in a Griggs-type apparatus on fine-grained aggregates of ordered schiller labradorite (An54) and of partly ordered clear, gem-quality Sonoran labradorite (An60). Single crystals of ordered An54 (containing <1 vol% ilmenite and biotite inclusions) and of pure An60 were ground. The 2–6 μm grain size fraction was separated by settling in water and dried at 120 °C. Pistons (6.35 mm in diameter and ~12 mm in length) were cored from partly ordered clear Sonoran labradorite (An60) single crystals and then cut at 45° to the long axis. Shallow grooves were cut into the 45° surfaces of the pistons to improve their coupling to the plagioclase sample. In all experiments ~70–80 mg of 2–6 μm labradorite powder was placed between the 45° cut plagioclase pistons inside a metal jacket. Experiments on An54 utilized a mechanically sealed inner Pt jacket and a thin outer Ni jacket; experiments on An60 utilized a weld-sealed Au inner jacket (except for the 750 °C experiment using "as-is" powder, which utilized a mechanically-sealed Pt-jacket) and a thin Ni outer jacket. In all experiments the end pistons were of ZrO_2 and the confining medium was NaCl.

The schiller (An54) "as-is" powder contains adsorbed H_2O as well as intracrystalline H_2O (in biotite); the total H_2O content was determined by weight loss after heating at 1,000 °C for 3 h to be 0.4 wt%. The Sonoran gem quality (An60) "as-is" powder contains only adsorbed H_2O (determined by the same method to be 0.1 wt%). Given some variability of water adsorption, the H_2O content of the Sonoran (An60) "as-is" samples should be at most between 0.1 and 0.2 wt%. In samples of schiller (An54) "as-is" samples, not all of the biotite dehydrates; some biotite is always present after the experiments. Therefore, the H_2O content available for reaction is less than 0.4 wt% in the schiller (An54) "as-is" samples. Water contents of 0.1 and 0. 4 wt% should consume ~10 and ~40% of the anorthite component of the starting material An60, respectively.

In order to compare the microstructures and strengths of reacted and unreacted samples at 750 °C, 1.5 GPa, water had to be removed from some samples to suppress the zoisite-forming hydration reaction. To obtain dried samples, ordered (An54) labradorite powder (with biotite inclusions) was pre-heated between the plagioclase pistons and inside the unsealed jackets at 1,000 °C under atmospheric conditions for 3 h to break down hydrous phases. (However, later examination of deformed samples showed that some biotite remained.) All heat-treated ordered (An54) as well as partly ordered (An60) samples, inside their unsealed jackets, were kept at 700 °C under vacuum for 18 h to 3 days to remove adsorbed water. After this heat treatment, Pt-jackets were mechanically sealed and Au-jackets were weld-sealed.

The samples were first hot-pressed in the Griggs apparatus for 12 h at 900 °C and 1 GPa (in the plagioclase stability field), producing an aggregate of deformed and partly recrystallized grains with <1% porosity. The hot-pressed plagioclase aggregate forms

a layer approximately 0.5 mm thick between the labradorite pistons. Deformation was performed at either 750 °C, 1.5 GPa (zoisite stability field) or at 900 °C, 1 GPa (plagioclase stability field, Fig. 1a) at a shear strain rate of 5×10^{-5} s^{-1}. After the motor was turned on, samples remained hydrostatic for an additional ~9 h before deformation commenced. Two hydrostatic experiments were performed to evaluate the microstructures and reaction progress in the absence of deformation. These samples were prepared (using "as-is" powder) in the same way as for the deformation experiments and then held at 750 °C, 1.5 GPa for 24 h (the time to achieve a shear strain of γ=1 to 2).

Examination of the samples was carried out using light as well as scanning (SEM) and transmission (TEM) electron microscopy. Phases were identified by energy dispersive X-ray (EDS) analysis in the SEM and TEM and electron diffraction in the TEM. Quantitative estimates of the plagioclase composition of reaction products were made in the SEM and TEM by comparing count ratios (background corrected) of Al/(Al+Si) of product and starting material plagioclase, using the known composition of the starting material as a standard. Estimation of the modal zoisite content of samples was carried out on thresholded binary SEM-backscatter-images using NIH-Image software.

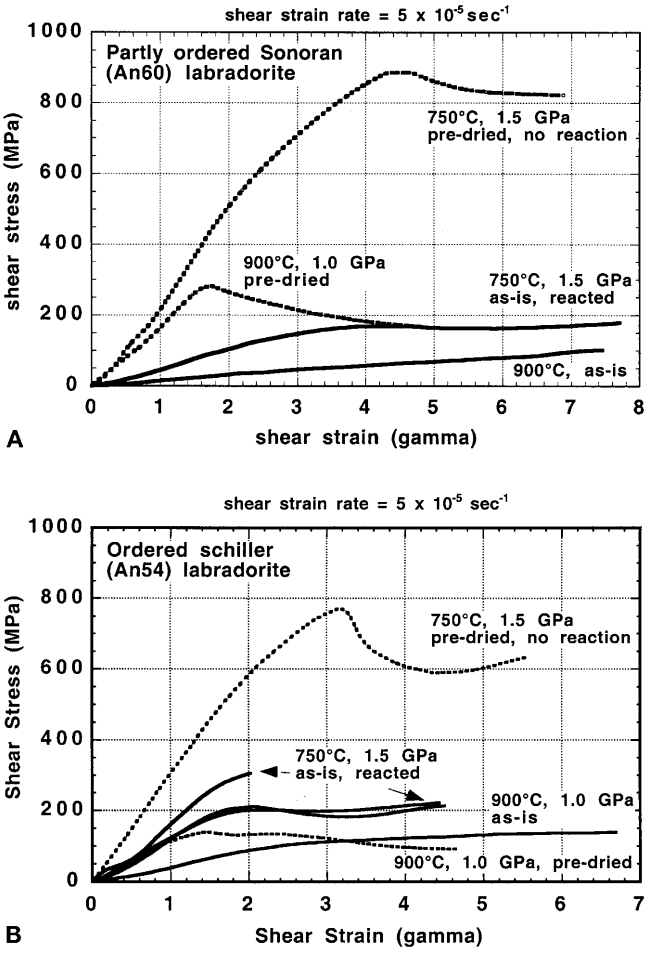

Fig. 2 Mechanical data for samples deformed in shear. Pre-dried samples are shown with *dotted lines*, "as-is" samples with *solid lines*. **A** Partly ordered Sonoran (An60) plagioclase samples. **B** Ordered schiller (An54) samples. Three experiments on "as-is" labradorite at 750 °C, 1.5 GPa are plotted: two experiments to a shear strain of approximately γ=4.5, and one that was stopped at the first signs of decreasing hardening behavior (~γ=2)

Results

Mechanical data

The experiments at 900 °C, 1 GPa (in the intermediate plagioclase stability field, no reaction) show consistent differences in mechanical behavior between "as-is" and pre-dried samples (Fig. 2a,b). The pre-dried partly ordered Sonoran labradorite (An60) has a peak strength of almost 300 MPa at low strain and then strain weakens to ~170 MPa (Fig. 2a). In contrast, the "as-is" sample has a barely discernible yield strength but gradually hardens. The difference in mechanical behavior between pre-dried and "as-is" samples of the ordered schiller labradorite (An54) at 900 °C, 1 GPa is similar to that of Sonoran (An60) samples (Fig. 2b), but not as pronounced.

For samples deformed at 750 °C, 1.5 GPa (in the zoisite stability field), there are substantial differences in mechanical behavior of the dry (unreacted) and the "as-is" (reacted) samples. The mechanical data for partly ordered Sonoran (An60) and ordered schiller (An54) labradorite samples are quite similar (Fig. 2a, b). The dry (unreacted) samples have a very high peak strength (differential stress approximately equal to confining pressure), followed by some weakening and approximately steady state flow at a high stress (Fig. 2a, b). The "as-is" samples deformed with concurrent reaction have a much lower peak strength followed by approximately steady state flow (Fig. 2a,b). The strength of the two high strain reacted samples is quite reproducible (180–200 MPa, Fig. 2a, b), and is similar to that of unreacted pre-dried partly ordered (An60) plagioclase deformed at 150 °C higher temperature. The "as-is" sample deformed to γ=2 (Fig. 2b) has a higher peak strength than the other reacted samples; we are not sure of the reason for this.

Microstructures

The microstructures of the partly ordered (An60) and ordered (An54) plagioclases deformed at 900 °C, 1.0 GPa (in the plagioclase stability field) are essentially the same. In both the dry and the "as-is" samples the deformation is distributed homogeneously throughout the shear zone. TEM shows that relict pla-

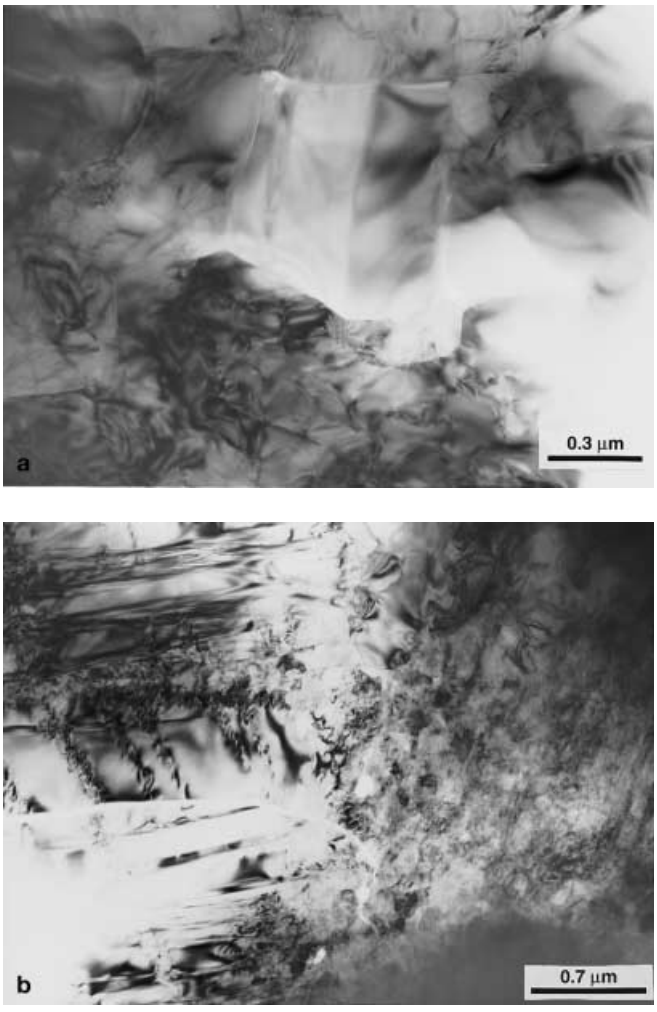

Fig. 3 Deformation microstructures of samples deformed at 900 °C, 1.0 GPa and pre-dried samples deformed at 750 °C, 1.5 GPa. **a** TEM image of recrystallized grains in ordered (An54) labradorite sample, deformed at 900 °C, 1.0 GPa, "as-is". The grain in the center is dislocation-free, others have variable dislocation densities. **b** TEM image of pre-dried ordered (An54) sample deformed at 750 °C, 1.5 GPa (no reaction). Microfractures in the twinned relict grain (left) are decorated with dislocations. The grain to the right shows a region of cataclasis and another region with a very high dislocation density

gioclase grains contain high dislocation densities and many twins; the dislocation densities are generally higher in the pre-dried samples. Small new recrystallized grains (grain size ~1 μm) usually are free of dislocations or have variable dislocation densities (Fig. 3a). No systematic change in An content could be detected by EDS between the relict and new grains in the TEM or from backscatter contrast and EDS in the SEM. This observation indicates that no chemical reaction occurred during recrystallization of plagioclase, consistent with the predicted phase relations (Fig. 1). The microstructures are indicative of regime 1 dislocation creep (Hirth and Tullis 1992), which involves strain induced grain boundary migration recrystallization as the recovery process because dislocation climb is difficult.

The microstructures of the pre-dried ordered (An54) and partly ordered (An60) samples deformed at 750 °C, 1.5 GPa (in the zoisite stability field) are also very similar to each other. Deformation is again distributed homogeneously throughout the shear zone, and no zoisite was detected. TEM shows that some relict plagioclase grains have very high dislocation density tangles, some have dislocations along microfractures, and some contain zones of cataclasis (Fig. 3b). The relict grains have been partially replaced by new recrystallized grains with low dislocation densities, a size of 0.1 to 0.5 μm, and no detectable change in An content. The extent of recrystallization varies strongly from virtually none to locally up to 50%. The microstructures in the pre-dried samples deformed at 750 °C, 1.5 GPa are somewhat similar to those of the pre-dried samples deformed at 900 °C, 1.0 GPa, but the lower temperature samples have fewer and considerably smaller recrystallized grains (compare Fig. 3b,c), and a far greater abundance of microfractures. These microstructures are consistent with deformation that is transitional from semi-brittle flow to regime 1 dislocation creep.

Five experiments were carried out at 750 °C, 1.5 GPa on "as-is" samples in order to determine the mechanical effects of the reaction and to study the microstructural development from undeformed samples to high shear strains. Two samples (ordered An54) were hydrostatic (24 h in the zoisite field), one (An54) was deformed to a shear strain of γ=2, two (An54) were deformed to a shear strain of γ=4.5, and one (partly ordered An60) was deformed to a shear strain of γ=7.5.

The hydrostatic samples contain aggregates of large prismatic zoisite grains (up to 50 μm long), which are randomly oriented or occur in radiating clusters, set in a matrix of fine-grained plagioclase (Fig. 4a). All of the deformed samples also contain aggregates of large zoisite grains. However, all of the "as-is" samples held or deformed in the zoisite stability contain unanticipated reaction products. First, small (~5-μm length) grains of white mica (mostly K-mica, only rare Na-mica) are dispersed throughout, and kyanite is only present in trace amounts (only identified in the TEM). Second, original plagioclase grains have developed rims of recrystallized grains that are more albitic. The An-content of these new plagioclase grains is An34–36 in both Sonoran and schiller plagioclase samples (determined by analytical SEM and TEM). Consequently, the reaction observed in these deformed samples is: An60 (or An54) + H_2O → An34–36 + zoisite + white mica + quartz + kyanite. The presence of white mica and albitic plagioclase indicates that the water content in these samples was locally >0.8 wt% (see Fig. 1c).

The sample deformed to γ=2 (Fig. 2b) shows no strain localization; it contains aggregates of large zoisite grains (10–20 μm diameter, 100–400 μm long)

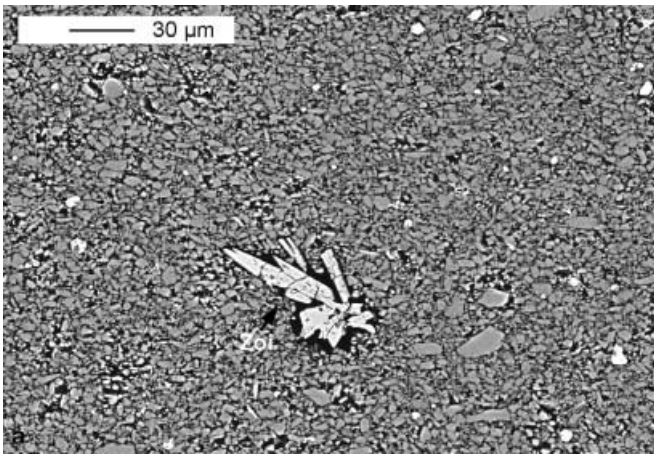

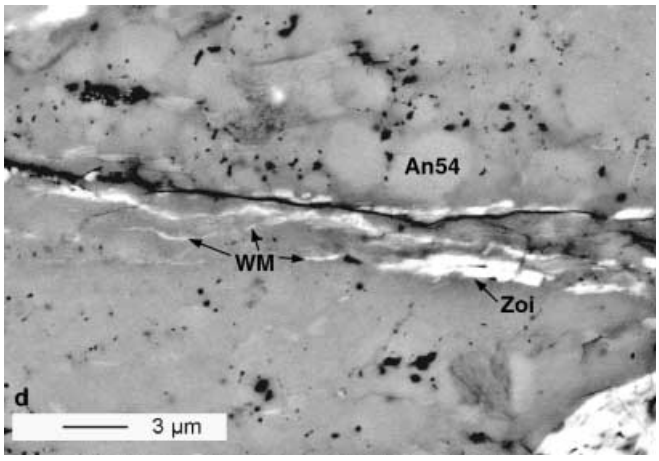

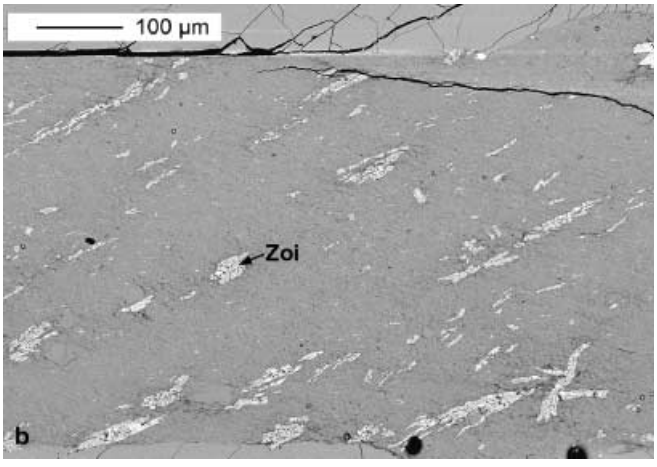

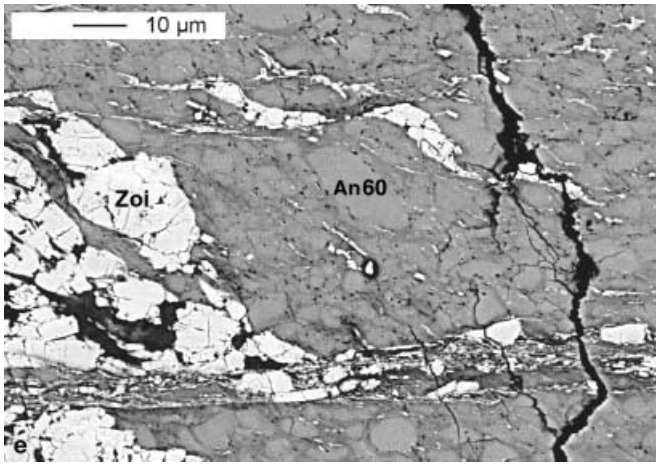

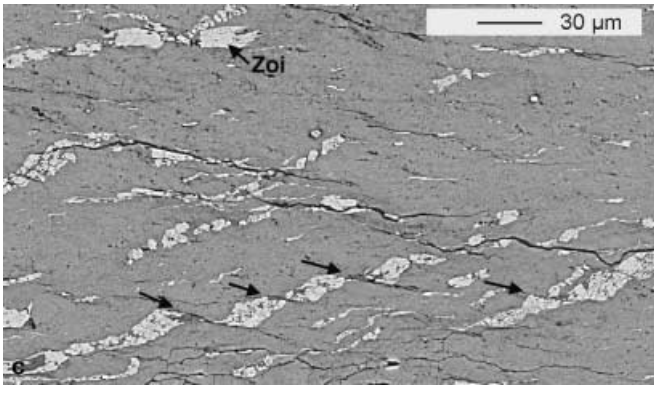

Fig. 4 Deformation and reaction microstructures of "as-is" samples deformed at 750 °C, 1.5 GPa. **a** SEM-backscatter image of a sample held hydrostatically at 750 °C, 1.5 GPa for 24 h. The acicular, large zoisite crystals (*light gray*) form randomly oriented to radiating aggregates within the ordered An54 schiller labradorite matrix (*medium gray*). **b** SEM backscatter image of ordered (An54) labradorite deformed to a shear strain of γ=2. Shear sense is dextral, the shear plane is horizontal. At the upper and lower margins of the image, the Sonoran (An60) piston material is visible (partly fractured because of sample unloading after the experiment). The *light gray* phase is zoisite, which occurs as large grains and aggregates aligned parallel to the extension direction of the shear zone. The darker, mottled regions are areas with rims of more albitic (An34–36) plagioclase around original (An54) plagioclase and finely dispersed reaction phases (not visible because of low magnification). **c** SEM backscatter image of the shear zone deformed to γ=4.5 in ordered (An54) schiller labradorite (one of the two experiments in Fig. 2b). The shear plane is horizontal in the image and shear sense is dextral. The large zoisite aggregates initially grew in the extension direction of the shear zone, but are now offset along synthetic shear bands (marked by *arrows*) at an angle of ~15 to 20° to the shear plane. The matrix consists of the intermediate (An54) plagioclase with albitic recrystallized rims and finely dispersed reaction phases (*light*). The shear bands consist of more albitic (An34–36) plagioclase and form dark lines because of the lower contrast in SEM-backscatter. **d** Detail of a shear band from **c** (running ~east–west in the center of the image). There are rims of more albitic (An34–36, *darker contrast*) plagioclase around the original (An54) labradorite grains in the matrix. The same, more albitic (An34–36) plagioclase composition is also found in the shear bands. Note the extremely fine grain size of white mica, zoisite, and (An34–36) plagioclase in the shear band. **e** SEM backscatter image of matrix and shear band (lower third of image) in partly ordered (An60) Sonoran labradorite (750 °C, 1.5 GPa "as-is" experiment in Fig. 2a). Shear sense is sinistral, and the shear plane is horizontal. The more albitic (An34–36) recrystallized rims (*dark gray*) surround original plagioclase (An60) grains in a core–mantle structure. The approximately horizontal shear band in the lower part of the image is wider than usual (10–15 µm) and consists of the same more albitic (An34–36) plagioclase (*dark*), zoisite and white mica (*light gray/white*)

most of which are oriented with their long axes approximately in the direction of finite extension (Fig. 4b). These coarse aggregates nucleated and began to grow during the ~9 h the sample was hydrostatic in the zoisite field before deformation began. However, the zoisite aggregates are considerably larger than those in the hydrostatic samples, and the shear strain is not high enough to have produced their strong preferred orientation by passive rotation of randomly oriented rigid particles in a deforming matrix. In addition, quartz is observed in dilatant sites in some of the large, oriented zoisite grains. These microstructures indicate that the zoisite underwent preferred growth and some fracturing during this low strain stage of deformation. In the matrix of this sample the rims of albitic recrystallized grains and the dispersed white mica grains are much more noticeable than they are in the hydrostatic sample.

The three samples deformed to higher strain (γ=4.5 and 7.5) are characterized by spectacular strain localization, in both ordered An54 and partly ordered An60. The high strain samples contain large zoisite grains and aggregates whose size and configuration are identical to those in the lower strain (γ=2) sample. However, these large grains have been cross-cut and synthetically offset along very narrow (1–3 μm) shear bands that make an angle of ~15–25° to the shear zone boundaries (Fig. 4c). In samples of both An54 and An60, the shear bands consist of very small grains of zoisite and more albitic plagioclase together with some white mica and very subordinate kyanite (Fig. 4d). In the matrix of both samples, outside the shear bands, there is a core-mantle structure of more albitic recrystallized rims around the original plagioclase grains, as in the lower strain (γ=2) sample (Fig. 4d, e).

TEM observations of the high strain samples show that the matrix consists of relict original plagioclase grains (several μm in diameter) with twins and high dislocation densities. The relict grains are replaced at their margins by very fine (0.2–1 μm diameter; Fig. 5a) new plagioclase grains that are more albitic (An34–36) than the starting material and have low dislocation densities or are dislocation-free. The fact that the new grains have a different composition from the starting material indicates that "recrystallization" involved nucleation of plagioclase with a new composition (thus better termed neocrystallization) as well as local grain boundary migration driven partly by strain energy and partly by chemical disequilibrium (CIGM or DIGM, Evans et al. 1986; Hay and Evans 1987a,1987b). The

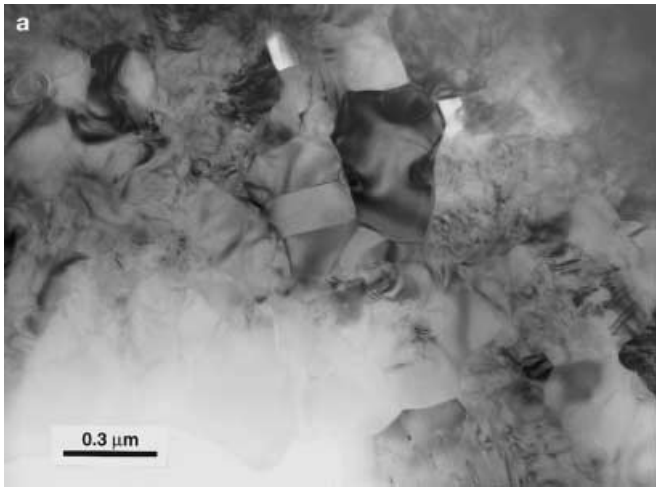

Fig. 5 **a** TEM image of ordered "as-is" (An54) labradorite deformed at 750 °C, 1.5 GPa to γ=4.5 showing recrystallized plagioclase grains in the matrix of the sheared sample. The grains with high dislocation densities are portions of the old grains, and the dislocation-free grains are new grains that have more albitic (An34–36) composition than the starting material. **b** TEM image of a shear band in ordered (An54) labradorite (extending horizontally between the arrowheads), consisting of zoisite (*dark laths*) and albitic plagioclase (*small grains next to triangles*). Most of the grains within the shear band are dislocation-free, and zoisite grains are well aligned with the shear band boundaries. Recrystallized matrix plagioclase is observed above and below the shear band; note the coarser grain size

microstructures indicate that regime 1 dislocation creep occurred, but the fact that the porphyroclasts and recrystallized grains have different chemical compositions indicates that the rate of recrystallization was probably enhanced. The coarse-grained zoisite aggregates in the matrix do not appear to have undergone internal deformation and contain few if any dislocations.

The narrow shear bands of extremely fine-grained reaction products have accommodated most of the sample strain after γ=2 (the sample deformed to γ=2 has not developed shear bands), and their microstructures are strikingly different from those of the matrix. TEM shows that the plagioclase grains within the shear bands are considerably smaller (0.02-0.1 μm) than those in the matrix, and they are always dislocation-free (Fig. 5b). These grains have the same composition (An34–36) as the new plagioclase grains in the matrix outside the shear bands, indicating that they also formed by heterogeneous nucleation. New grains of zoisite and white mica are mixed with the An34–36 plagioclase; they are dislocation-free and are well-aligned with the shear band boundaries (Fig. 5b). The presence of very small, dislocation-free grains (zoisite, white mica and plagioclase) is typical for deformation by diffusion-accommodated grain boundary sliding.

Summarizing, samples deformed without reaction at 900 °C, 1.0 GPa and 750 °C, 1.5 GPa show homogeneous deformation, whereas samples deformed with concurrent reaction at 750 °C, 1.5 GPa show pronounced strain localization into narrow shear bands composed of extremely fine-grained reaction products. Furthermore, the appearance of these shear bands at a shear strain of $\gamma \geq 2$ coincides with the onset of approximately steady state flow at a much lower stress than occurs in the absence of reactions.

Discussion

The actual phase assemblage produced in the 750 °C, 1.5 GPa experiments on "as-is" An54 and An60 samples with 0.1 wt% H_2O is white mica + An34–36 plagioclase + zoisite + kyanite + quartz. This assemblage differs from that calculated (for An60) at these conditions (zoisite + An57 plagioclase + kyanite + quartz; Fig. 1b) by the presence of white mica and a much lower An content. The observed white mica corresponds to the assemblage calculated for a higher H_2O content (>0.8 wt% H_2O at 1.5 GPa; Fig. 1c), and indicates H_2O-saturated conditions (excess H_2O in the equilibrium assemblage). We have calculated a P–T diagram for a H_2O content of 1 wt% (Fig. 1e, f), which would be sufficient to react the entire sample to an equilibrium assemblage. Fig. 1e shows that the absence of white mica at these H_2O conditions would require higher temperatures (although these would result in melting according to the experiments of Goldsmith (1982); Fig. 1a). The calculated equilibrium An content of the plagioclase at 1.5 GPa and 1 wt% H_2O is An29 (Fig. 1d, f), which is in good agreement with the observed An content of new plagioclase grains (An34–36). The observed assemblage most likely represents local equilibrium, associated with locally H_2O-saturated conditions, initially along grain boundaries and later along the shear bands. Thus, on the scale of the experimentally deformed samples, bulk equilibrium is not attained and the local equilibrium corresponds to much higher H_2O contents than the bulk H_2O content. A multi-stage reaction history of zoisite-forming reactions because of episodes of fluid infiltration during generally H_2O-undersaturated conditions has been inferred for natural gabbroic rocks by Wayte et al. (1989) and Rubie (1990b).

The difference in strength between pre-dried and "as-is" samples deformed at 900 °C, 1.0 GPa in the plagioclase stability field (Fig. 2a,b) occurs almost certainly because of H_2O weakening of the samples with a trace of moisture. H_2O weakening in the dislocation creep regime is best documented for quartz deformed by climb-accommodated dislocation creep (e.g., Paterson 1989; Post et al. 1993), but has also been observed in feldspar (Tullis and Yund 1980) for recrystallization-accommodated dislocation creep. For this process, the principal effect of the water is probably to enhance the rate of grain boundary migration (e.g., Tullis and Yund 1989), thus facilitating the recovery step. The most likely explanation why the schiller (An54) samples have a smaller difference in strength between the pre-dried and "as-is" samples than the Sonoran (An60) samples is that the decomposition of hydrous phases in the schiller (An54) samples in the pre-drying procedure is incomplete. Hydrous phases (e.g., biotite) may partially decompose during the experiment and release H_2O.

There are three possible reasons for the difference in strength between the pre-dried and "as-is" samples deformed at 750 °C, 1.5 GPa: (1) an enhanced rate of grain boundary migration recrystallization of the plagioclase matrix resulting from H_2O weakening; (2) an enhanced rate of recrystallization (actually neocrystallization) of the plagioclase matrix resulting from the additional driving potential because of compositional disequilibrium; and (3) a change in deformation mechanism from regime 1 dislocation creep to diffusion-accommodated grain boundary sliding within the fine-grained reaction products in the shear bands. Trace amounts of water increase the rate of grain boundary migration (e.g., Tullis and Yund 1989) and chemical free energy increases the driving potential for grain boundary migration (CIGM; Evans et al. 1986; Hay and Evans 1987a,1987b). Both factors thus tend to enhance the rate of recovery during low temperature dislocation creep. One or both of these factors must be responsible for the lower strength of the 'as-is' Sonoran (An60) sample deformed to γ=2 at 750 °C, 1.5 GPa, compared with the pre-dried sample

deformed at the same conditions (Fig. 2b), because the γ=2 sample contains no localized shear bands. However, in the samples deformed to shear strains of γ=4.5 to 7.5, almost all of the sample strain beyond γ>2 has been accomplished by deformation within multiple very narrow shear bands containing extremely fine-grained and dislocation-free reaction products. For the steady state flow stress of these experiments (200 MPa) the strain rate within the narrow shear bands was obviously much faster than that within the plagioclase matrix. Thus, the strength of this fine-grained polyphase assemblage of reaction products must be significantly lower than that of the plagioclase matrix. We infer this low strength is caused by a switch in deformation mechanism from dislocation creep to diffusion-accommodated grain boundary sliding.

There are several observations indicating that the deformation mechanism within the fine-grained shear bands was diffusion-accommodated grain boundary sliding, rather than a different weakening process. First, the weakening behavior associated with the reaction is not transient because the stress–strain curves show steady state flow from the point of initiation of the shear bands (γ~2) up to strains of γ=7.5 (Fig. 2b). This behavior indicates that the weakening is not caused by a type of transformation plasticity, which would be associated with the reaction process itself and, thus, would be a transient phenomenon or would have to involve a moving reaction front (Poirier 1982; Meike 1993). Water weakening of the plagioclase does occur, as is shown by the mechanical data for the 900 °C, 1.0 GPa experiments in Sonoran (An60) plagioclase. However, this effect and that of chemically-enhanced grain boundary migration appear to be less important than the switch in deformation mechanism within the shear bands because the offsets of large zoisite grains clearly indicate that once the shear bands form they accommodate most of the sample strain. One of the phases in the shear bands is white mica, which is known to be a weak phase that deforms easily by crystal plasticity (Shea and Kronenberg 1992, 1993; Mares and Kronenberg 1993). However, mica as a weak phase does not appear to control the deformation in the shear bands because the micas are dislocation-free, do not show subgrains or grain boundary migration features, and are well dispersed in the very fine-grained phase mixture rather than forming interconnected layers. These observations are not consistent with crystal plastic deformation of white mica being a dominant deformation mechanism in the shear bands. Instead, the microstructural relations indicate that the shear bands have deformed by diffusion-accommodated grain boundary sliding: the material within the shear bands has accomplished very high strains, at high strain rates, and yet it has remained extremely fine-grained and dislocation-free.

The mechanism for the initiation of the shear bands is not clear. One possibility to consider is that the shear bands developed along brittle faults induced by pore fluid pressure. However, the shear bands only form after a substantial volume of zoisite has been produced by the reaction. If the observed reaction goes to completion, the amount of H_2O present in the sample (0.1 wt%) is sufficient to produce 4.2 vol% zoisite. The estimated volume fraction of zoisite in the sample deformed to γ=2 is 4.3–4.9 vol%. Although this is only an approximate value, it demonstrates that most of the zoisite that can be produced in the experiment is present before the shear bands initiate. Therefore, most of the H_2O has been consumed before the shear bands form, and the pore pressure must be much lower than at the start of the experiment. Thus, a brittle initiation of the shear bands because of pore pressure is very unlikely.

Although it is difficult to prove, we infer that the shear bands form by coalescence of small regions of locally greater reaction progress. The presence of white mica and albitic (An34–36) plagioclase indicates that the H_2O content in the deformed samples was locally >0.8 wt% (Fig. 1c). If the H_2O was distributed inhomogeneously, the reaction products may not have been uniformly distributed. Because small patches of reaction products are weaker as a result of a switch in deformation mechanism, then the enhanced deformation rate might lead to further reaction in their vicinity. Eventually these patches might coalesce into through-going shear bands, perhaps cutting across pre-existing large zoisite grains at points of quartz infilling.

In an earlier study (Rutter and Brodie 1988b), very fine-grained reaction products in shear bands were observed in dehydration deformation experiments on serpentinite, and the mechanical weakening observed in these samples was also attributed to a switch in deformation mechanism from dislocation creep to diffusion-accommodated grain boundary sliding. The fine-grained deformation zones of Rutter and Brodie (1988b) consist of single phase olivine. Single-phase aggregates with a very fine grain size are likely to undergo grain growth. Thus, the weakening effect associated with grain size reduction resulting from dynamic recrystallization (Schmid 1982; Handy 1989) or reactions that produce single-phase aggregates (Rutter and Brodie 1988a) is likely to be a transient phenomenon in nature because grain growth would tend to switch the deformation mechanism back to dislocation creep. The shear bands in our plagioclase samples consist of a phase mixture (plagioclase, zoisite, white mica, and kyanite), in which grain growth is strongly inhibited. The inhibition of grain growth in phase mixtures resulting from reactions is likely to persist even at slower strain rates and, therefore, can be expected to result in a long-term weakening of the rock.

There are far more fine-grained reaction products in the "as-is" sample deformed at 750 °C, 1.5 GPa to γ ~2 than in samples kept at hydrostatic conditions for

the same time. This observation indicates a higher nucleation rate during deformation compared with hydrostatic conditions, a result that is in accord with many observations in naturally deformed rocks (e.g., Brodie and Rutter 1985; Klaper 1990) where reaction progress is more complete in high strain zones than in undeformed portions of the rock. The higher nucleation rate of reaction products during deformation may result from several factors. Deformed material generally has a smaller grain size because of dynamic recrystallization, which provides more grain boundary sites for heterogeneous nucleation. In addition, high dislocation densities are probably important. In nature it is common to find new plagioclase grains that differ in composition from their host by An10. The ΔG associated with this compositional difference is the same as that resulting from a dislocation density of 10^{10} cm^{-2} (Stunitz 1998), which is a commonly observed value in deformed plagioclase. Thus the ΔG for nucleation and boundary migration is effectively doubled in deformed material with high defect densities.

In nature, the hydration reaction plagioclase → more albitic plagioclase + Ca–Al-silicate (and other phases) takes place over a wide temperature range in all lithologies containing plagioclase if aqueous fluids are present. The rapid nucleation, which is enhanced by deformation, makes the reaction a very common feature, especially in shear zones. Microstructural relations suggest that this reaction causes strong localization of deformation in rocks naturally deformed under greenschist facies conditions (Stünitz 1993; Stünitz and Fitz Gerald 1993). The fine grain size of the reaction products in jadeite-bearing phase mixtures in localized deformation zones described by Rubie (1983) might also occur because of the rapid nucleation of the Ca–Al-silicates. Thus, the plagioclase-zoisite reaction may initiate an important weakening mechanism during the deformation of plagioclase-containing rocks. The reaction is dependent upon aqueous fluid infiltration because it is a hydration reaction. Fluid infiltration takes place most easily along cracks and microfractures so that brittle deformation (common in plagioclase in greenschist-facies rocks) may be an important precursor to diffusion-accommodated grain boundary sliding in naturally deformed rocks if hydration reactions are involved.

Our experiments document the strain weakening effect of reactions through enhanced nucleation of product phases and the resulting phase mixtures that lead to stable fine-grained assemblages. Heterogeneous nucleation is a very effective mechanism for grain size reduction. It is driven by a combination of strain energy plus chemical instability of solid solution phases in an assemblage. Because most rock-forming minerals are solid solution phases, their equilibrium composition is likely to change along any given P,T-path during their tectonic history. An example of this effect is described by Newman et al. (1999) for solid–solid sliding reactions in a mantle rock, although in their case the reaction progress does not depend on infiltrating fluids as it does for hydration reactions. In general, reaction-driven recrystallization or neocrystallization is a very common process in polyphase rocks during deformation and may lead to considerable grain size refinement, which may induce a switch in deformation mechanism to diffusion-accommodated grain boundary sliding. Such a switch in deformation mechanism can be a major cause for strain localization.

Conclusions

Hydration reactions in aggregates of intermediate plagioclase (An54 and An60) during deformation at H_2O-undersaturated conditions produce an assemblage of zoisite + An34–36-plagioclase + white mica + kyanite + quartz. This assemblage is at equilibrium at much higher H_2O contents than the bulk H_2O content, indicating that local equilibrium was at H_2O-saturated conditions. The shear deformation experiments show that samples undergoing syn-deformational reaction are significantly weaker than unreacted (dry) plagioclase aggregates deformed at the same conditions. The most important reason for the weakening is a switch in deformation mechanism from dislocation creep to diffusion-accommodated grain boundary sliding, which takes place in extremely fine-grained phase mixtures of the reaction products, localized along discrete and very narrow shear bands that form at low strain and accommodate most of the subsequent sample strain. The phase mixture inhibits grain growth and thus produces a stable fine-grained microstructure, which is necessary for steady state deformation and thus long-term weakening of the rock. This same reaction is observed in nature, where it is commonly associated with extreme strain localization. Our experiments suggest that syn-deformational reactions are likely to cause weakening and thus strain localization. Thus, localization of deformation in polyphase rocks may be favored by any P,T path where the equilibrium composition of the constituent minerals changes so that heterogeneous nucleation of new grains takes place.

Acknowledgements This work was supported by NSF EAR 9628348 and Swiss Nationalfonds Project 2000-055420.98. We have benefited from many discussions with Dick Yund. Christian de Capitani and Thorsten Nagel helped with the thermodynamic calculations, and Marcel Duggelin and Dani Mathys helped with the SEM work. Bill Collins made the thin sections and Sebastian Potel provided last minute help. We thank all of them very much for their contributions. The text has been improved substantially thanks to thorough reviews by Julie Newman and Dave Rubie.

References

Berman RG (1988) Internally consistent thermodynamic data for minerals in the system K_2O–Na_2O–CaO–MgO–FeO–Fe_2O_3–Al_2O_3–SiO_2–TiO_2–H_2O–CO_2. J Petrol 29:445–522

Boullier AM, Gueguen Y (1975) SP-mylonites: origin of some mylonites by superplastic flow. Contrib Mineral Petrol 50:93–104

Brodie KH, Rutter EH (1985) On the relationship between deformation and metamorphism with special reference to the behaviour of basic rocks. In: Thompson AB, Rubie DC (ed) Metamorphic reactions: kinetics, textures, and deformation. Advances in physical geochemistry, vol 4. Springer, Berlin Heidelberg New York, pp 138–179

Chatterjee ND, Froese E (1975) A thermodynamic study of the pseudobinary join muscovite–paragonite in the system $KAlSi_3O_8$–$NaAlSi_3O_8$–Al_2O_3–SiO_2–H_2O. Am Miner 60:985–993

Cumbest RJ, Drury MR, van Roermund HLM, Simpson C (1989) Dynamic recrystallization and chemical evolution of clinoamphibole from Senja, Norway. Contrib Mineral Petrol 101:339–349

de Capitani C, Brown TH (1987) The computation of chemical equilibrium in complex systems containing non-ideal solutions. Geochim Cosmochim Acta 51:2639–2652

de Capitani C (1994) Gleichgewichtsphasendiagramme: Theorie und Software. Eur J Miner 6:48–50

Evans B, Hay RS, Shimizu N (1986) Diffusion-induced grain boundary migration in calcite. Geology 14:60–63

Fitz Gerald JD, Stünitz H (1993) Deformation of granitoids at low metamorphic grades. I. Reactions and grain size reduction. Tectonophysics 221:269–297

Fueten F, Robin P-YF (1992) Finite element modelling of the propagation of a pressure solution cleavage seam. J Struct Geol 14:953–962

Fuhrman ML, Lindsley DH (1988) Ternary-feldspar modeling and thermometry. Am Mineral 73:201–215

Goldsmith JR (1982) Plagioclase stability at elevated temperatures and water pressure. Am Mineral 67:653–675

Handy MR (1989) Deformation regimes and the rheological evolution of fault zones in the lithosphere: the effects of pressure, temperature, grain size and time. Tectonophysics 163:119–152

Handy MR (1990) The solid-state flow of polymineralic rocks. J Geophys Res 95(B):8647–8661

Hay RS, Evans B (1987a) Chemically induced grain boundary migration in calcite: temperature dependence, phenomenology, and possible applications to geological systems. Contrib Mineral Petrol 97:127–141

Hay RS, Evans B (1987b) Chemically induced grain boundary migration in low and high angle calcite boundaries. Acta Metall 35:2049–2062

Hirth G, Tullis J (1992) Dislocation creep regimes in quartz aggregates. J Struct Geol 14:145–159

Jordan PG (1987) The deformation behaviour of bimineralic limestone-halite aggregates. Tectonophysics 135:185–197

Kerrich R, Allison J, Barnett RL, Moss S, Starkey J (1980) Microstructural and chemical transformations accompanying deformation of granite in a shear zone at Miéville, Switzerland; with implications for stress corrosion cracking and superplastic flow. Contrib Mineral Petrol 73:221–242

Klaper E (1990) Reaction enhanced formation of eclogite shear zones in granulite facies anorthosites. Geol Soc Lond Spec Publ 54:167–173

Mares VM, Kronenberg AK (1993) Experimental deformation of muscovite. J Struct Geol 15:1061–1075

Meike A (1993) A critical review of investigations into transformation plasticity. In: Boland JN, Fitz Gerald JD (ed) Defects and processes in the solid state: geoscience applications. Elsevier, Amsterdam, pp 5–25

Mitra G (1978) Ductile deformation zones and mylonites: the mechanical processes involved in the deformation of crystalline basement rocks. Am J Sci 278:1057–1084

Murrell SAF, Ismail IAH (1976) The effect of the decomposition of hydrous minerals on the mechanical properties of rocks at high pressures and temperatures. Tectonophysics 31:207–235

Newman J, Lamb WM, Drury MR, Vissers RLM (1999) Deformation processes in a peridotite shear zone: reaction-softening by an H_2O-deficient, continuous net transfer reaction. Tectonophysics 303:193–222

Olgaard DL, Ko SC, Wong TF (1995) Deformation and pore pressure in dehydrating gypsum under transiently drained conditions. Tectonophysics 245:237–248

Paterson MS (1989) The interaction of water with quartz and its influence in dislocation flow – an overview. In: Karato S-I, Toriumi M (ed) Rheology of solids and the earth. Oxford University Press, New York, pp 107–142

Poirier JP (1982) On transformation plasticity. J Geophys Res 87:6791–6797

Post A, Tullis J, Yund RA (1993) Effects of chemical environment on dislocation creep of quartzite. J Geophys Res 101:22143–22155

Raleigh CB, Paterson MS (1965) Experimental deformation of serpentinite and its tectonic implications. J Geophys Res 70:3965–3985

Rubie DC (1983) Reaction-enhanced ductility: the role of solid-solid univariant reactions in deformation of the crust and mantle. Tectonophysics 96:331–352

Rubie DC (1990a) Mechanisms of reaction enhanced deformability in minerals and rocks. In: Barber DJ, Meredith PG (ed) Deformation processes in minerals, ceramics and rocks. Unwin Hyman, London, pp 262–295

Rubie DC (1990b) Role of kinetics in the formation and preservation of eclogites. In: Carswell DA (ed) Eclogite facies rocks. Blackie, Glasgow, pp 111–140

Rutter EH, Brodie KH (1988a) The role of tectonic grain size reduction in the rheological stratification of the lithosphere. Geol Rundsch 77:295–308

Rutter EH, Brodie KH (1988b) Experimental "syntectonic" dehydration of serpentinite under conditions of controlled pore water pressure. J Geophys Res 93:4907–4932

Schmid SM (1982) Microfabric studies as indicators of deformation mechanisms and flow laws operative in mountain building. In: Hsü KJ (ed) Mountain building processes. Academic Press, London, pp 95–110

Shea WT, Kronenberg AK (1992) Rheology and deformation mechanisms of an anisotropic mica schist. J Geophys Res 97(B):15201–15237

Shea WT, Kronenberg AK (1993) Strength and anisotropy of foliated rocks with varied mica contents. J Struct Geol 15:1097–1121

Stünitz H (1993) Transition from fracturing to viscous flow in a naturally deformed metagabbro. In: Boland JN, Fitz Gerald JD (ed) Defects and processes in the solid state: geoscience applications. Elsevier, Amsterdam, pp 121–150

Stünitz H (1998) Syndeformational recrystallization: dynamic or compositionally induced? Contrib Mineral Petrol 131:219–236

Stünitz H, Fitz Gerald JD (1993) Deformation of granitoids at low metamorphic grades. II. Granular flow in albite-rich mylonites. Tectonophysics 221:299–324

Tullis J, Wenk HR (1994) Effect of muscovite on the strength and lattice preferred orientation of experimentally deformed quartz aggregates. Mater Sci Eng A175:209–220

Tullis J, Yund RA (1980) Hydrolytic weakening of experimentally deformed Westerly granite and Hale albite rock. J Struct Geol 2:439–451

Tullis J, Yund RA (1985) Dynamic recrystallization of feldspar: a mechanism for ductile shear zone formation. Geology 13:238–241

Tullis J, Yund RA (1989) Hydrolytic weakening of quartz aggregates: the effects of water and pressure on recovery. Geophys Res Lett 16:1343–1346

Tullis J, Yund RA (1992) The brittle–ductile transition in feldspar aggregates: an experimental study. In: Evans B, Wong TF (eds) Fault mechanics and transport properties in rocks. Academic Press, New York, pp 89–118

Tullis J, Dell'Angelo LN, Yund RA (1990) Ductile shear zones from brittle precursors in feldspathic rocks; the possible role of dynamic recrystallization. In: Duba A, Durham W, Handin J, Wang H (ed) The brittle–ductile transition: the Heard volume 56. Am Geophys Monogr, Washington, DC, pp 67–82

Tullis TE, Horowitz F, Tullis J (1991) Flow laws of polyphase aggregates from end member flow laws. J Geophys Res 96:8081–8096

Wayte GJ, Worden RH, Rubie DC, Droop GTR (1989) A TEM study of disequilibrium plagioclase breakdown at high pressure: the role of the infiltrating fluid. Contrib Mineral Petrol 101:426–437

Wheeler J (1992) Importance of pressure solution and Coble creep in the deformation of polymineralic rocks. J Geophys Res 97:4579–4586

White SH, Knipe RJ (1978) Transformation- and reaction-enhanced ductility in rocks. J Geol Soc Lond 135:513–516